CHAPTER ONE
INTRODUCTION

1.1 Background of Study

This project is about the study of corroded pipelines used in the oil and gas industry. Pipelines function as the most reliable and economical way of transmitting medium from one point to another, therefore the safety of these pipelines is paramount to ensure unintended failure. One of the main reasons of pipeline failure is due to corrosion defects; therefore this matter has to be investigated to ensure the pipeline operates safely and economically. This project also involves the studies of available codes related to corroded pipelines, such as the ASME B31G and the DNV-RP-F101. These codes are used as reference to determine the failure pressure of the pipelines based on simulations with the ANSYS software.

1.2 Problem Statement

Corrosion defects are known to be one of the major reasons for pipeline failure. Pipelines failures include pipelines leaking and bursting, causing fatalities. The number of accidents and critical issues regarding the preservation of the environment has also been dramatically increased with the increasing number of operating pipelines. The integrity of these transmitting pipelines is of the importance due to the explosive characteristics of oil and gas. For these reasons, intensive research efforts have been carried out on the assessment of structural integrity of pipelines. Regular inspections have to be done to assess the rate of change of physical conditions of pipes, which gives more accurate idea on how much longer a pipeline can be expected to operate safely and productively.

One of the tests carried out to assess the structural integrity of pipelines is the burst test. A pipe will be pressure tested to burst to obtain the Maximum Allowable Burst Pressure (P_b). Therefore with this method the integrity of the pipeline can be determined. Burst test cannot be conducted to every pipeline to assess the structural

integrity due to time, money and safety constraints. Therefore, an alternative is to simulate the burst test, as it is economical and safe. The results of numerical analysis and burst test simulations using ANSYS software are then compared to the experimental values.

1.3 Objectives

The objectives of this project are:

a) to determine the Maximum Allowable Burst Pressure (P_b) of corroded pipelines using the Finite Element Analysis (FEA).
b) to compare and correlate the numerical analysis with the experimental values as well as determining the best model for simulation of corroded pipelines using ANSYS software.

1.4 Scope of Study

This project is to assess the integrity of corroded pipeline subjected to internal pressure loading by using the Finite Element Analysis (FEA) method. The software, ANSYS will be used in this study to generate the 3-D models. A pipe segment will be pressure tested to burst by using simulations to determine its pressure resistance and the results are compared to the experimental results.

CHAPTER TWO
LITERATURE REVIEW

Currently, many experts and engineers are conducting intensive research to evaluate the integrity of the corroded pipelines and the failure predictions. Therefore, there are many codes available for assessing the integrity of corroded pipelines, such as ASME B31G and DNV-RP-F101. These codes were based on extensive series of full scale tests on corroded pipelines sections and they provide guidance for assessing the integrity of corroded pipelines. Researches are still being conducted to determine the best approach of evaluating the burst test of corroded pipelines.

A paper on the development of limit load solutions for corroded gas pipelines was written based on a series of burst test performed on X65 gas pipelines with mechanically machined corrosion defects [1]. As a result, a Fitness-For-Purpose (FFP) type of limit load solutions is proposed based on experimental results and Finite Element Analysis (FEA) [1]. The comparison of burst pressure between burst test and Finite Element Analysis for API X65 steel pipe is shown in **Figure 2.1** [1]. A reference stress for failure prediction was determined by comparing FEA results with burst test results, resulting the following:

a) The reference stress for failure prediction of rectangular corrosion pit is determined to be 90% of ultimate strength, and that for elliptical corrosion pit is 80% of ultimate strength.
b) A FFP type limit load solution for the assessment of corrosion pit in X65 gas pipelines is proposed as a function of the normalised parameters based on the corrosion pit geometry:

$$P_{max} = \frac{2t}{D_i}\sigma_o\left[A_2\left(\frac{l}{\sqrt{Rt}}\right)^2 + A_1\left(\frac{l}{\sqrt{Rt}}\right) + A_0\right]$$

Where;

$$\sigma_o = \sigma_u$$

$$A_2 = 0.01163\left(\frac{a}{t}\right)^2 - 0.1053\left(\frac{a}{t}\right) + 0.0292$$

$$A_1 = -0.2676\left(\frac{a}{t}\right)^2 - 0.0187\left(\frac{a}{t}\right) - 0.007$$

$$A_0 = 0.0617\left(\frac{a}{t}\right)^2 - 0.0268\left(\frac{a}{t}\right) + 1.001$$

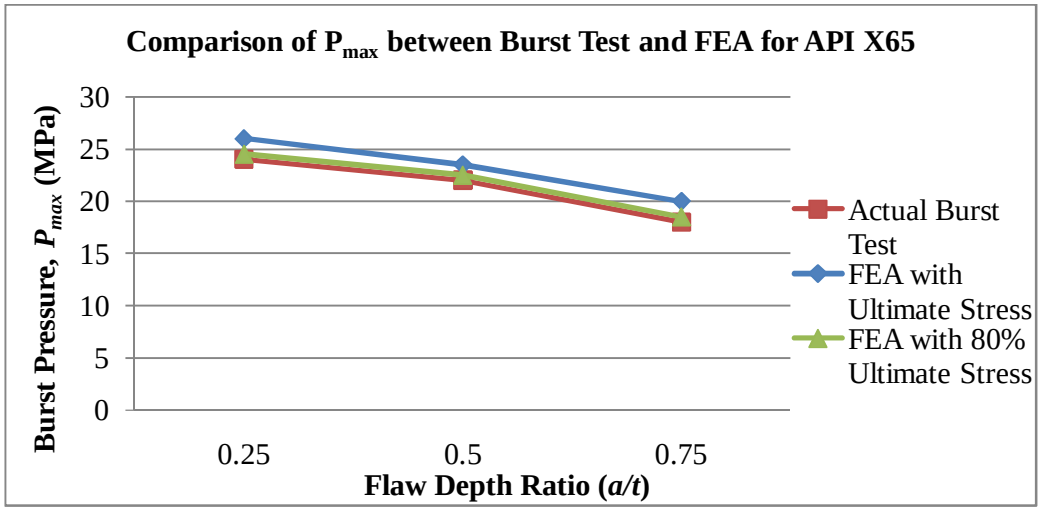

Figure 2.1: Comparison of P_{max} between Burst Test and FEA for API X65

In a research paper of automatic finite element solid modelling, burst test and error analyses of corroded pipelines, the researchers presented a new program, named PIPE. PIPE can be used to automatically generate and solve solid models of pipe [2]. The PIPE program provides a friendly Graphical User Interface (GUI) for the ANSYS Software allowing a guided and quick modeling of pipes containing multiple different defects in arbitrary position. A validation test was presented showing that the program leads to an appropriate model generation and to a reliable numerical simulation [2]. This paper also provides the comparisons between Finite Element Analysis results and the available codes; ASME B31G, RSTRENG 0.85dl, and the DNV codes. The results are tabulated as shown in **Table 2.1**.

Table 2.1: Actual and Predicted Failure Pressures and Corresponding Errors

Method	Failure Pressure (MPa)	Error (%)
Burst Test	21.26	0
FEM	20.91	-1.65
ASME B31G	17.76	-16.48
RSTRENG 0.85*dl*	16.73	-21.30
DNV	18.72	-11.97

Another research paper is about the comparison of experimental results and computations for cracked tubes subjected to internal pressure using three available methods [3]. These methods are ASME B31G, modified ASME B31G and DNV RP- F101. In this paper, it can be concluded that it is difficult to construct a meshed structure that represents notched pressure pipe [3]. The results, however, from the Finite Element computations give consistent results with respect to experimental data [3]. The experimental results are compared; it seems that the ASME B31G code is the closest, whilst the DNV code is the most conservative [3]. The comparisons of the results are tabulated as shown in **Table 2.2** [3].

Table 2.2: Different Ultimate Pressure and Error Comparisons

Codes	P_{ult}**/MPa**	**Error compared to experimental result (%)**
ASME B31 G	11.3	5.8
Modified ASME B31G	10.8	10.0
DNV RP-F101	6.6	45.0

CHAPTER THREE
METHODOLOGY

In order to accomplish this project, several steps are taken to develop the Finite Element Analysis simulations. The overall methodology is illustrated in a flow diagram form shown in **Figure 3.1** below.

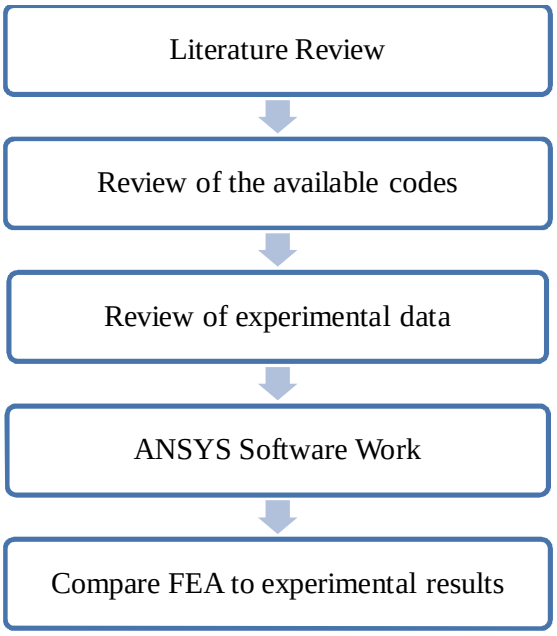

Figure 3.1: Methodology

3.1 Literature Review

The first part of the methodology is to understand the scope and the background of the project. Journals, theses and codes related to the project have to be studied and familiarized in order to analyze the project. Real-size pipelines experimental data are needed in order to simulate the models, and then the results from simulations will be compared to the experimental results.

3.2 Codes and Equations Review

The two codes that are widely used to evaluate the strength of the corroded pipes are ASME B31G and DNV-RP-F101. Therefore, in this project, these two codes are studied and used as guidelines to determine the Maximum Allowable Burst Pressure (P_b) from simulations.

3.2.1 ASME B31G

This code is intended for the purpose of providing guidance in the evaluation of metal loss in pressurized pipelines and piping systems. The equations in this manual were developed based upon pressuring actual corroded pipe to failure in an extensive series of full-size tests. It is applicable to all pipelines and piping systems that are part of ASME B31 Code for Pressure Piping. With this code, safe maximum pressure for corroded pipelines can be determined.

The steps for determining Maximum Allowable Operating Pressure are:

i) Computation of Projected Area of Corrosion, A

$$A = 0.893\left(\frac{L_m}{\sqrt{Dt}}\right) \qquad \text{(Eq. 1)}$$

ii) Computation of P

$$P = 2StFT / D \qquad \text{(Eq. 2)}$$

iii) Computation of Safe Maximum Pressure, P'

$$P' = 1.1P\left[\frac{1-\frac{2}{3}\left(\frac{d}{t}\right)}{1-\frac{2}{3\left(\frac{d}{t\sqrt{\left(A^2+1\right)}}\right)}}\right] \qquad \text{(Eq. 3)}$$

where,

A	=	Projected area of corrosion in the longitudinal plane through the wall thickness (mm^2)
d	=	Depth of corroded region (mm)
L_m	=	Longitudinal length of corroded region (mm)
t	=	Uncorroded, measured, pipe wall thickness (mm)
D	=	Nominal outside diameter (mm)
P'	=	The safe maximum pressure for the corroded area
P	=	The greater of either the established MAOP (Maximum Allowable Operating Pressure)
S	=	Specified minimum yield strength **(SMYS)**
F	=	Appropriate design factor
T	=	Temperature derating factor from the appropriate B31 Code

3.2.2 DNV-RP-F101

The RP (Recommended Practice) gives recommendations for the assessment of corroded pipelines subject to internal pressure, and internal pressure combined with longitudinal compressive stresses and covers single defects, interacting defects and complex shaped defects. DNV-RP-F101 proposes two methods to find the failure pressure. The first method is named the partial safety factor, and the second is classified as the allowable stress design.

For this project, the equations of longitudinal corrosion defect subjected to internal pressure loading are used. Therefore the Maximum Allowable Corroded Pressure can be determined from:

i) Calculation of Maximum Acceptable Defect Depth *(d/t)**

$$(d/t)^{*} = (d/t)_{means} + \varepsilon_d StD[d/t] \qquad \text{(Eq. 4)}$$

ii) Calculation of Length Correction Factor, Q

$$Q = \sqrt{1 + 0.31\left(\frac{L}{\sqrt{Dt}}\right)^2} \qquad \text{(Eq. 5)}$$

iii) Calculation of Maximum Allowable Corroded Pressure, P_{corr}

$$p_{corr} = \gamma_m \frac{2tf_u}{(D-t)} \frac{(1-\gamma_d(d/t)^{*})}{\left(1-\frac{\gamma_d(d/t)^{*}}{Q}\right)} \qquad \text{(Eq. 6)}$$

where,

A_c = Projected area of corrosion in the circumferential plane through the wall thickness (mm^2)

p_{corr} = Allowable corroded pipe pressure of a single longitudinal corrosion defect under internal pressure loading (N/mm^2)

d = Depth of corroded region (mm)

L = Longitudinal length of corroded region (mm)

t = Pipe wall thickness (mm)

D = Nominal outside diameter (mm)

γ_m = Partial safety factor for longitudinal corrosion model prediction

γ_d = Partial safety factor for corrosion depth

Q = Length correction factor

f_u = Tensile strength to be used in design

ε_d = Factor for defining a fractile value for the corrosion depth

3.3 ANSYS Software

ANSYS Software is a finite element analysis code widely used in the computer-aided engineering (CAE) field. This software allows users to construct computer models of structures, machine components or systems, apply operating loads and other design criteria, and etc. It permits an evaluation of a design without having to build and destroy multiple prototypes in testing. This software has a variety of design analysis applications ranging from simple to complex modelling.

In this project, Pre-ANSYS learning will take place once the literature review and theories are completed. The learning will be from simple ANSYS application up to modelling of pipe burst test simulations. The simulations of the burst test will be conducted under internal pressure loading with varying generalized models, rather than conducting real-size costly burst test.

3.4 Gantt Chart

The Gantt Chart in **Figure 3.2** below illustrates the work breakdown and the schedule of this project.

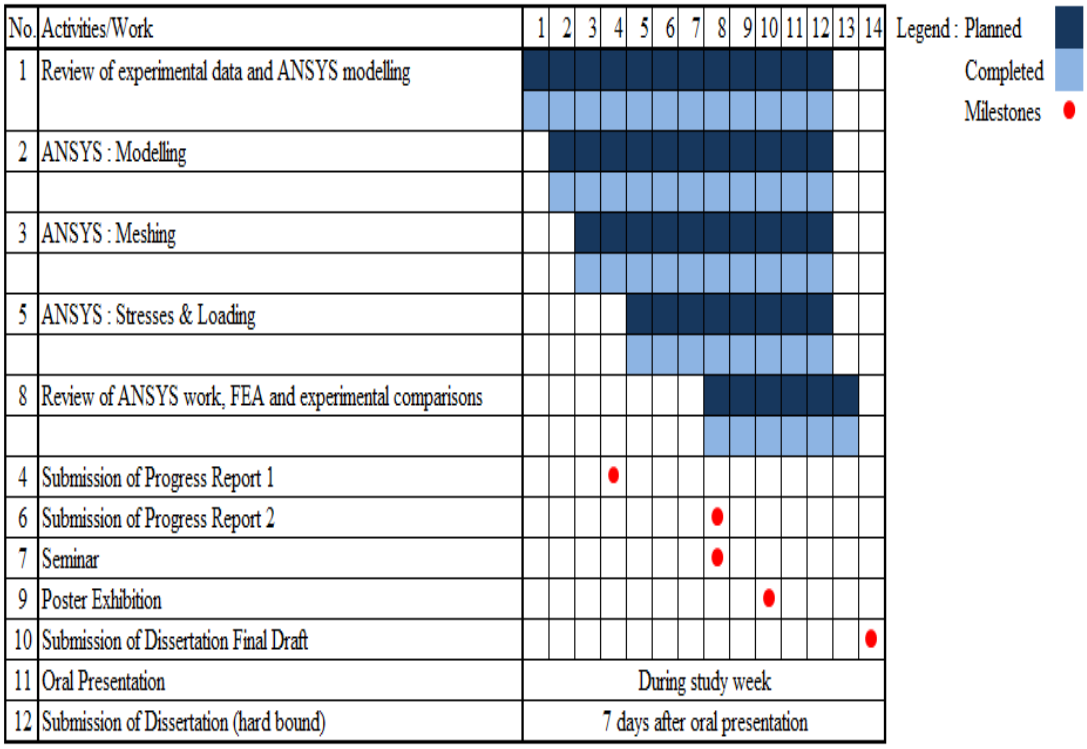

Figure 3.2: Gantt Chart

3.5 Experimental Data

In this project, the experimental data was taken from Universiti Teknologi PETRONAS (UTP) in-house burst test project. The experimental data of the pipe is illustrated in **Figure 3.3** and tabulated in **Table 3.1**.

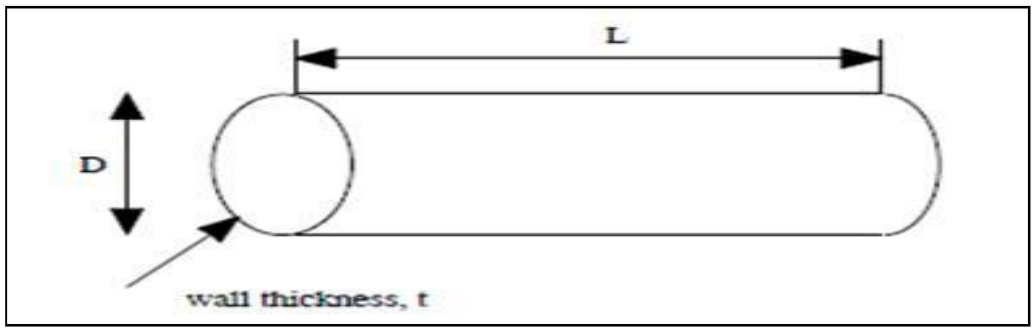

Figure 3.3: Dimensions of the Pipe

Table 4.1: Dimensions and Properties of the Pipe

Nominal Outide Diameter, *D*	274 mm
Wall thickness, *t*	12 mm
Length, *L*	2000 mm
Material Grade	API 5L X52
Specified Minimum Yield Strength, SMYS	358 MPa
Specified Minimum Tensile Strength, SMTS	455 MPa

The corroded pipe profile is measured and plotted in **Figure 3.4**, whereas the corroded pipe thickness is plotted in **Figure 3.5**.

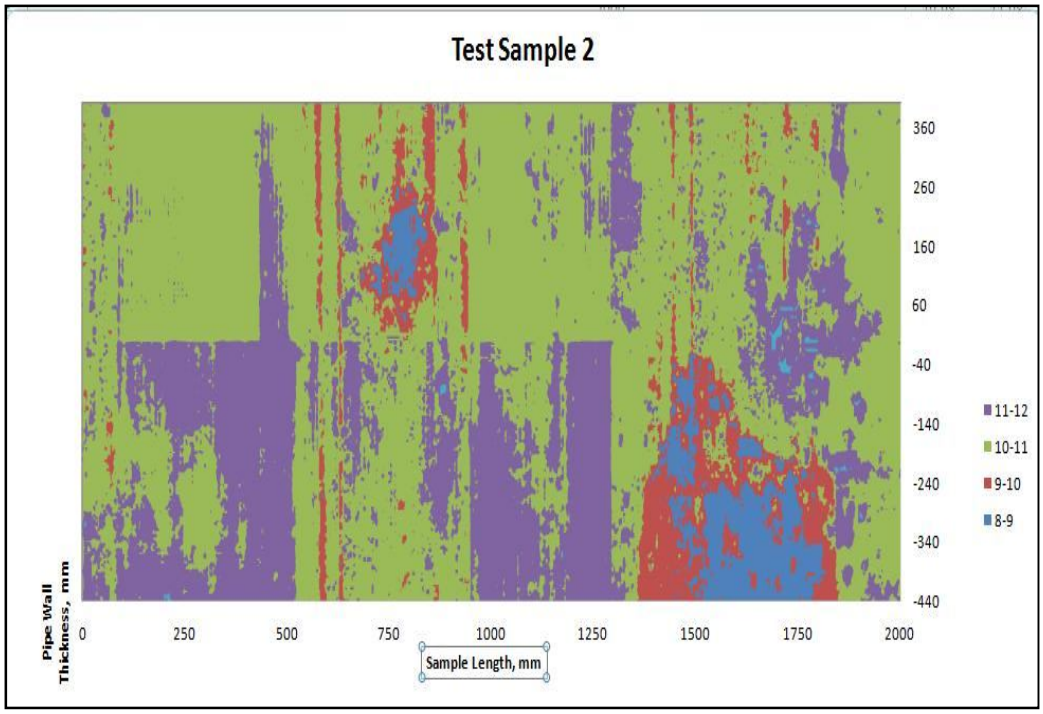

Figure 3.4: Corroded Pipe Profile Plot

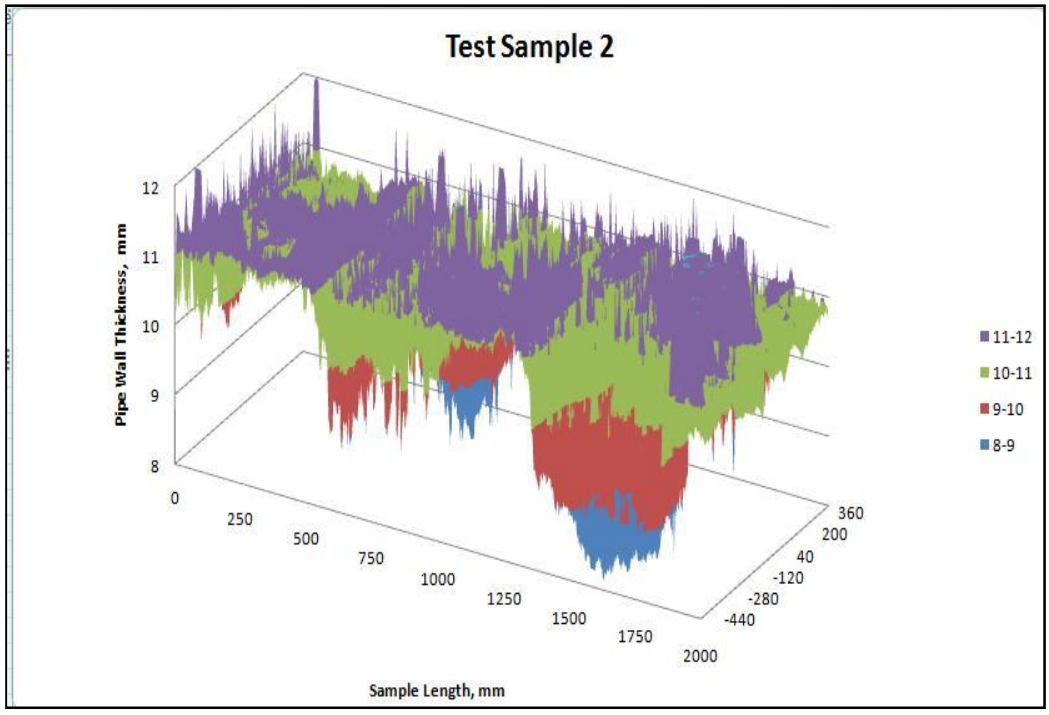

Figure 3.5: Corroded Pipe Thickness

3.6 Idealization

From the corroded pipe profile, the minimum thickness of the pipe also known as the deepest defect, is found as shown **Figure 3.6**.

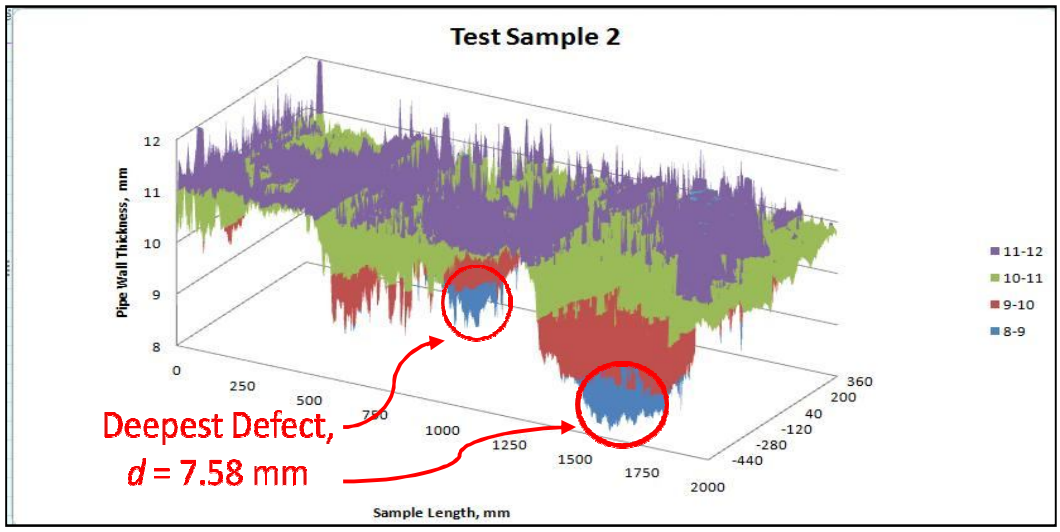

Figure 3.6: Deepest Defect on Pipe

By analyzing **Figure 3.4**, the corroded pipe profile is idealized as illustrated in **Figure 3.7** below. The idealized geometry of corrosion pits is shown in **Table 3.2**.

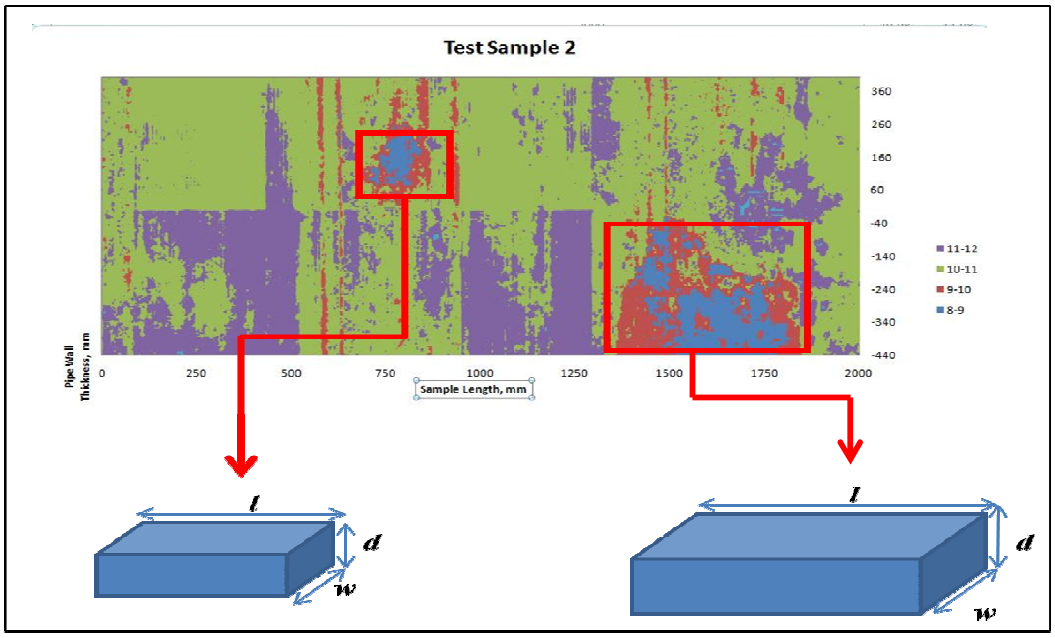

Figure 3.7: Idealization of Corroded Pipe Profile

Table 3.2: Idealized Geometry of Corrosion Pits

IDEALIZATION	GEOMETRY (A)	GEOMETRY (B)
Defect Depth, *d*	7.58 mm	7.58 mm
Length, *l*	200 mm	400 mm
Width, w	200 mm	400 mm

3.7 ANSYS Modelling and Meshing

After determining the geometry of the corrosion pits, the corroded pipe can be modelled in ANSYS. The models that are created and properly meshed for simulations are given in the following sub-sections.

3.7.1 Model 1: Average Defect Throughout

Model 1 is modelled using average defect depth throughout the whole length of the pipe as shown in **Figure 3.8**. The average defect depth throughout the pipe is obtained by averaging the corroded pipe profile in **Figure 3.5**. The dimensions for Model 1 are tabulated in **Table 3.3**.

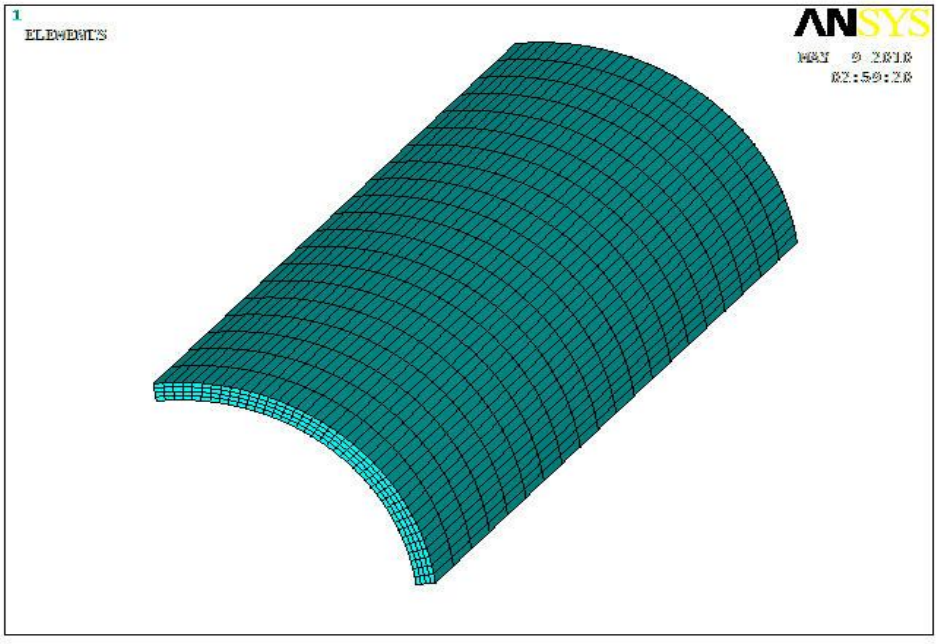

Figure 3.8: Average Defect Throughout

Table 3.3: Dimensions of Model 1

Dimensions	Real Geometry	FEA Symmetrical Model
Outer radius, r_o	137 mm	137 mm
Inner radius, r_i	125 mm	125 mm
Length, L	2000 mm	1000 mm
Defect depth, d	10.63 mm	10.63 mm

3.7.2 Model 2: External Defect Throughout, Width A

Model 2 is modelled by using the 200mm width and deepest defect depth, d using Geometry A (refer **Table 3.2**). The corrosion defect is modelled externally throughout the length of the pipe. Symmetry boundary conditions are applied to this model; as illustrated in **Figure 3.9** and the dimensions are tabulated in **Table 3.4**.

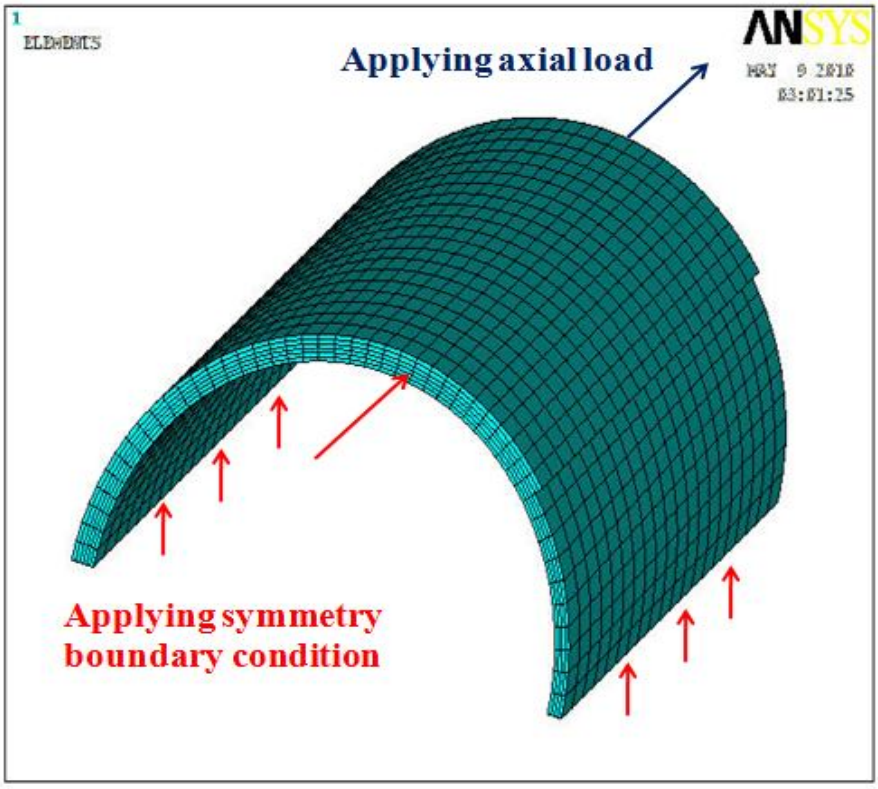

Figure 3.9: External Defect Throughout, Width A

Table 3.4: Dimensions of Model 2

Dimensions	Real Geometry	FEA Symmetrical Model
Outer radius, r_o	137 mm	137 mm
Inner radius, r_i	125 mm	125 mm
Length, L	2000 mm	1000 mm
Defect length, l	2000 mm	1000 mm
Defect depth, d	7.58 mm	7.58 mm
Defect width, w	200 mm	100 mm

3.7.3 Model 3: External Corrosion Pit, Geometry A

Model 3 is modelled with an external rectangular corrosion pit by using Geometry A. **Figure 3.10** shows Model 3 with an external corrosion pit and the dimensions of this model is tabulated in **Table 3.5**.

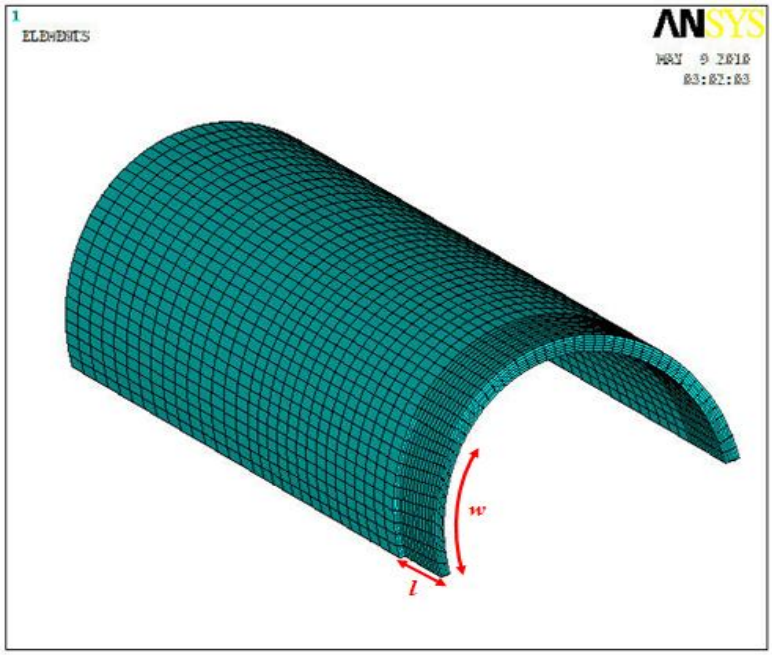

Figure 3.10: External Corrosion Pit, Using Geometry A

Table 3.5: Dimensions of Model 3

Dimensions	Real Geometry	FEA Symmetrical Model
Outer radius, r_o	137 mm	137 mm
Inner radius, r_i	125 mm	125 mm
Length, L	2000 mm	1000 mm
Defect length, l	200 mm	100 mm
Defect depth, d	7.58 mm	7.58 mm
Defect width, w	200 mm	100 mm

3.7.4 Model 4: Internal Corrosion Pit, Geometry A

Model 4 is modelled with an internal rectangular corrosion pit by using Geometry A. **Figure 3.11** shows Model 4 with an internal corrosion pit and the dimensions of this model is tabulated in **Table 3.6**.

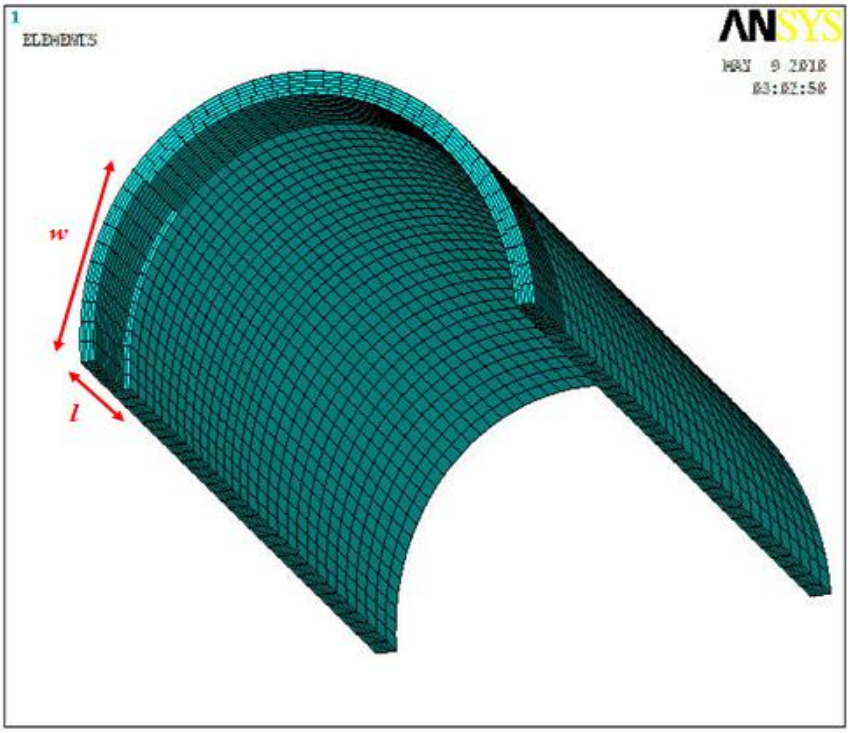

Figure 3.11: Internal Corrosion Pit, Using Geometry A

Table 3.6: Dimensions of Model 4

Dimensions	Real Geometry	FEA Symmetrical Model
Outer radius, r_o	137 mm	137 mm
Inner radius, r_i	125 mm	125 mm
Length, L	2000 mm	1000 mm
Defect length, l	200 mm	100 mm
Defect depth, d	7.58 mm	7.58 mm
Defect width, w	200 mm	100 mm

3.7.5 Model 5: External Defect Throughout, Width B

Model 5 is modelled by using the 400mm width and deepest defect depth, *d* using Geometry B (refer **Table 3.2**). The corrosion defect is modelled externally throughout the length of the pipe. Symmetry boundary conditions are applied to this model; as illustrated in **Figure 3.12** and the dimensions are tabulated in **Table 3.7**.

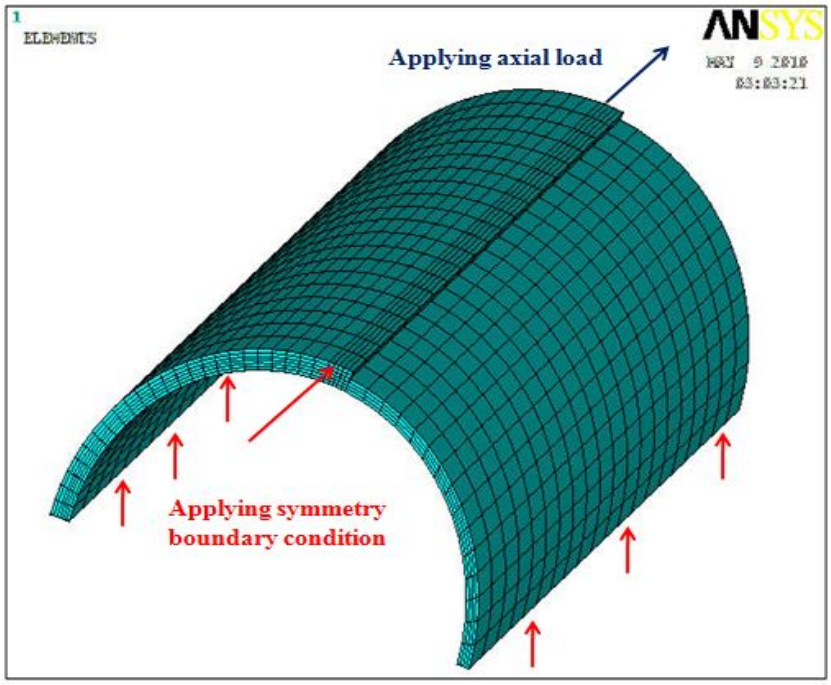

Figure 3.12: External Defect Throughout, Width B

Table 3.7: Dimensions of Model 5

Dimensions	Real Geometry	FEA Symmetrical Model
Outer radius, r_o	137 mm	137 mm
Inner radius, r_i	125 mm	125 mm
Length, L	2000 mm	1000 mm
Defect length, l	2000 mm	1000 mm
Defect depth, d	7.58 mm	7.58 mm
Defect width, w	400 mm	200 mm

3.7.6 Model 6: External Corrosion Pit, Geometry B

Model 6 is modelled with an external rectangular corrosion pit by using Geometry B. **Figure 3.13** shows Model 6 with an external corrosion pit and the dimensions of this model is tabulated in **Table 3.8**.

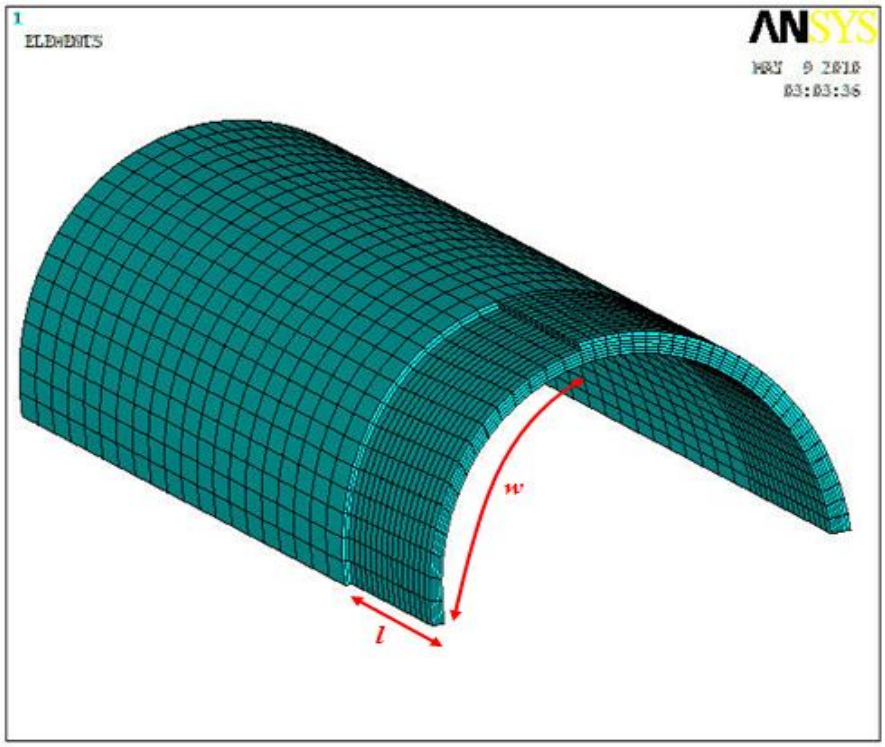

Figure 3.13: External Corrosion Pit, Using Geometry B

Table 3.8: Dimensions of Model 6

Dimensions	Real Geometry	FEA Symmetrical Model
Outer radius, r_o	137 mm	137 mm
Inner radius, r_i	125 mm	125 mm
Length, L	2000 mm	1000 mm
Defect length, l	400 mm	200 mm
Defect depth, d	7.58 mm	7.58 mm
Defect width, w	400 mm	200 mm

3.7.7 Model 7: Internal Corrosion Pit, Geometry B

Model 7 is modelled with an internal rectangular corrosion pit by using Geometry B. **Figure 3.14** shows Model 7 with an external corrosion pit and the dimensions of this model is tabulated in **Table 3.9**.

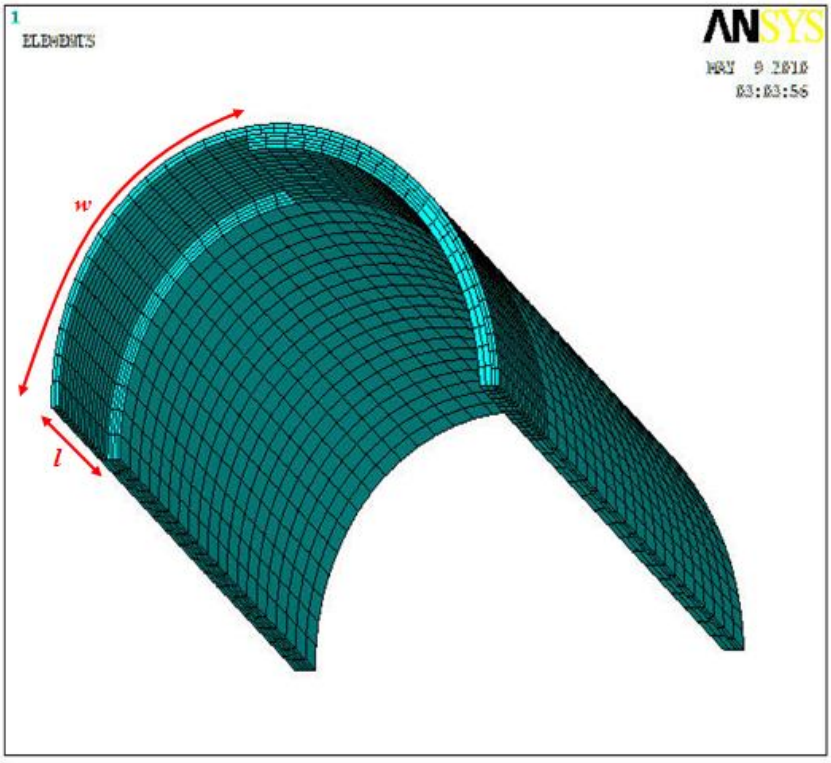

Figure 3.14: Internal Corrosion Pit, Using Geometry B

Table 3.9: Dimensions of Model 7

Dimensions	Real Geometry	FEA Symmetrical Model
Outer radius, r_o	137 mm	137 mm
Inner radius, r_i	125 mm	125 mm
Length, L	2000 mm	1000 mm
Defect length, l	400 mm	200 mm
Defect depth, d	7.58 mm	7.58 mm
Defect width, w	400 mm	200 mm

3.7.8 Model 8: External Rectangular Corrosion Pits, Geometry A and Geometry B

Model 8 is modelled symmetrically with two rectangular corrosion pits using Geometry A and Geometry B (refer Figure **3.7**). Modeling and meshing of Model 8 are as shown in **Figure 3.15** and **Figure 3.16** and the dimensions are tabulated in **Table 3.10**.

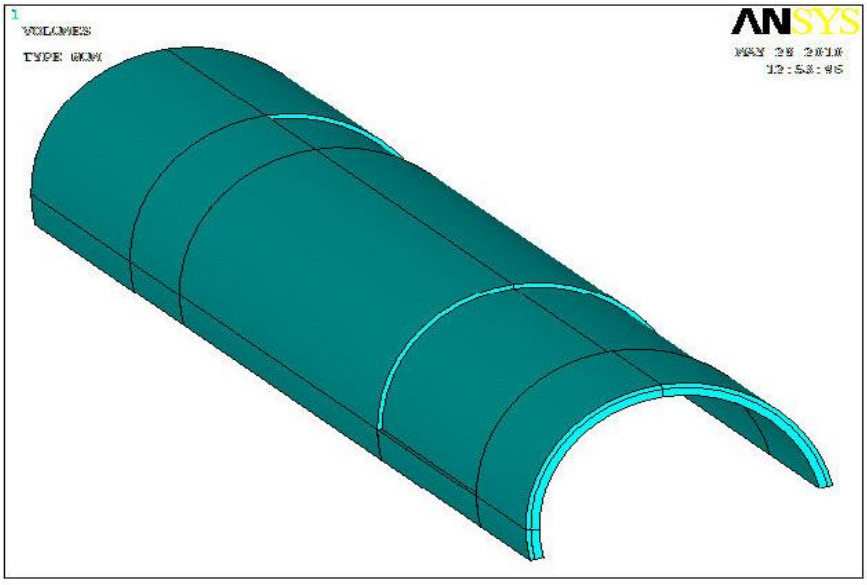

Figure 3.15: Modelling of Rectangular Corrosion Pits, Using Geometry A and B

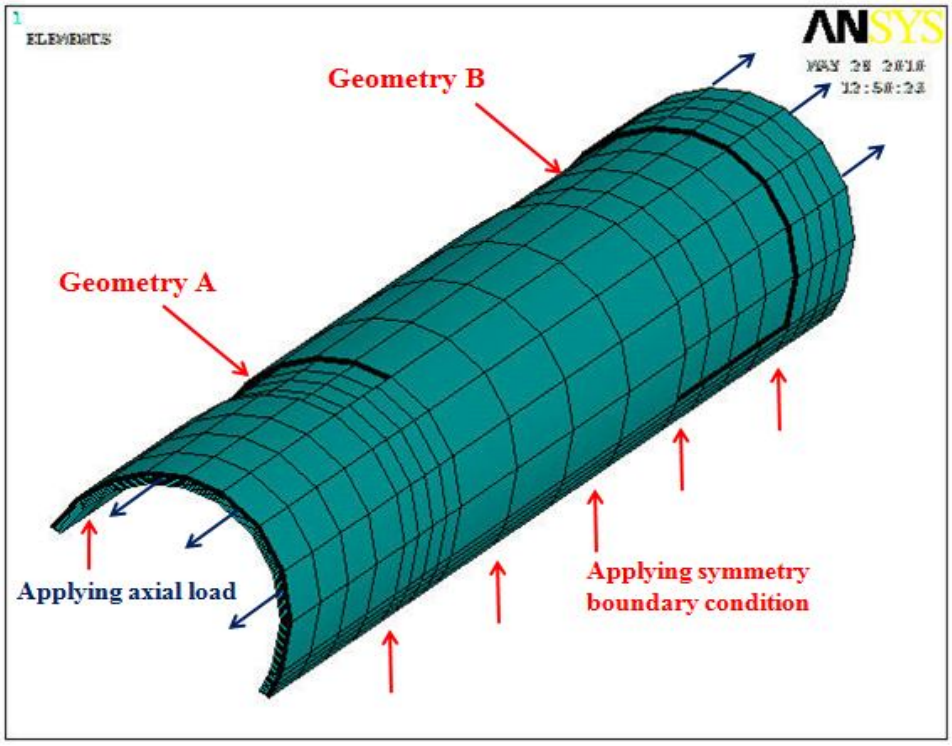

Figure 3.16: Meshing of Rectangular Corrosion Pits, Using Geometry A and B

Table 3.10: Dimensions of Model 8

Dimensions	Real Geometry	FEA Symmetrical Model
Outer radius, r_o	137 mm	137 mm
Inner radius, r_i	125 mm	125 mm
Length, L	2000 mm	2000 mm
Defect length, l_A	200 mm	200 mm
Defect depth, d_A	7.58 mm	7.58 mm
Defect width, w_A	200 mm	100 mm
Defect length, l_B	400 mm	400 mm
Defect depth, d_B	7.58 mm	7.58 mm
Defect width, w_B	400 mm	200 mm

3.8 ANSYS Simulations

After modelling and meshing, the models are then simulated by applying appropriate loadings and constraints. The steps involved in simulations of the corroded pipe are:

3.8.1 Applying Symmetry Boundary Conditions.

Since the pipe is modelled symmetrically, therefore the symmetry boundary conditions have to be applied on the models. **Figure 3.17** below illustrates the symmetry boundary conditions applied to Model 2.

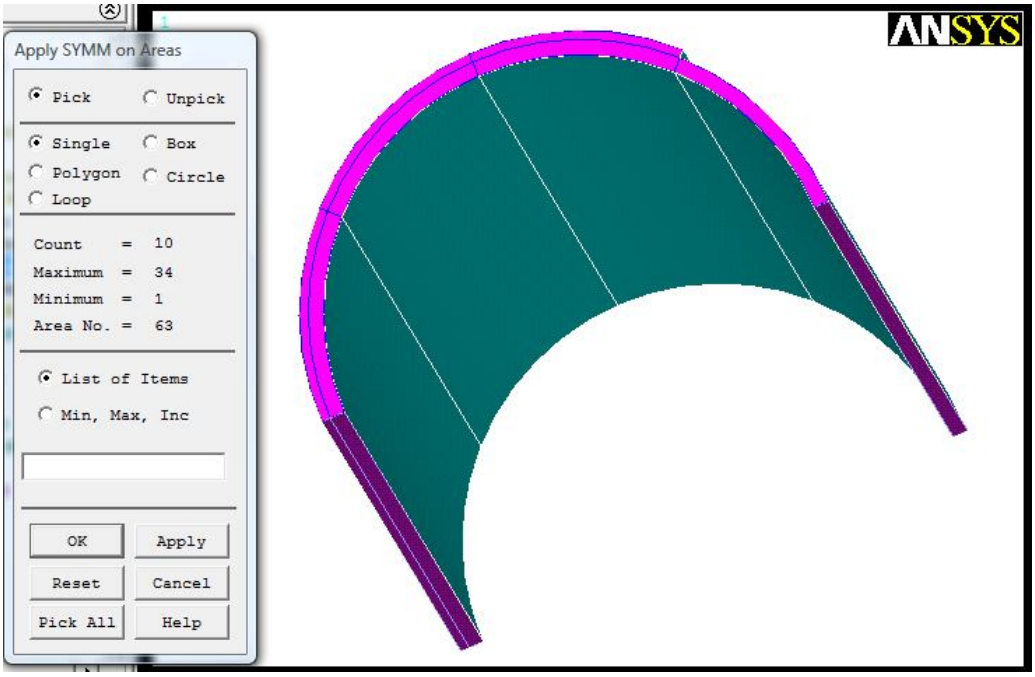

Figure 3.17: Applying Symmetry Boundary Conditions

3.8.2 Applying Axial Load, σ_{axial}

The axial load is dependent on the internal pressure loading, *P*. The axial load, σ_{axial} can be determined from the equation below:

$$\sigma_{axial} = \frac{P_{burst}(D)}{4t} \qquad \text{(Eq. 7)}$$

Figure 3.18 shows the application of axial load at the end of the model.

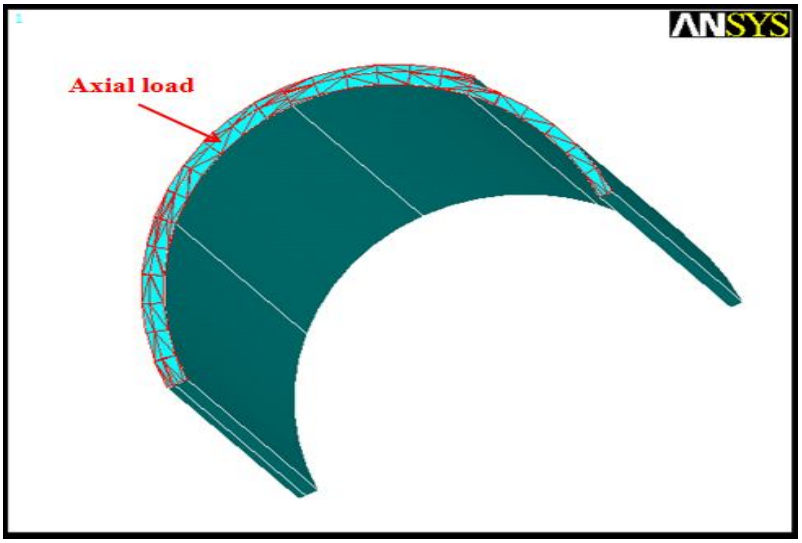

Figure 3.18: Applying Axial Load

3.8.3 Applying Internal Pressure Loading

The varying parameter for the models is the internal pressure loading, *P*. The prediction of failure pressure, P_{burst} can be calculated from ASME B31G (from **Eq. 1** to **Eq. 3**) and DNV-RP-F101 (from **Eq.4** to **Eq.6**). From the calculations of prediction of failure pressure, P_{burst}, the pressure is applied gradually to the internal area of the pipe, illustrated below in Figure **3.19** until the stress in the model reaches the ultimate tensile strength, σ_{uts}. The pressure value when the stress in the model is equal to σ_{uts} is considered as P_{burst}.

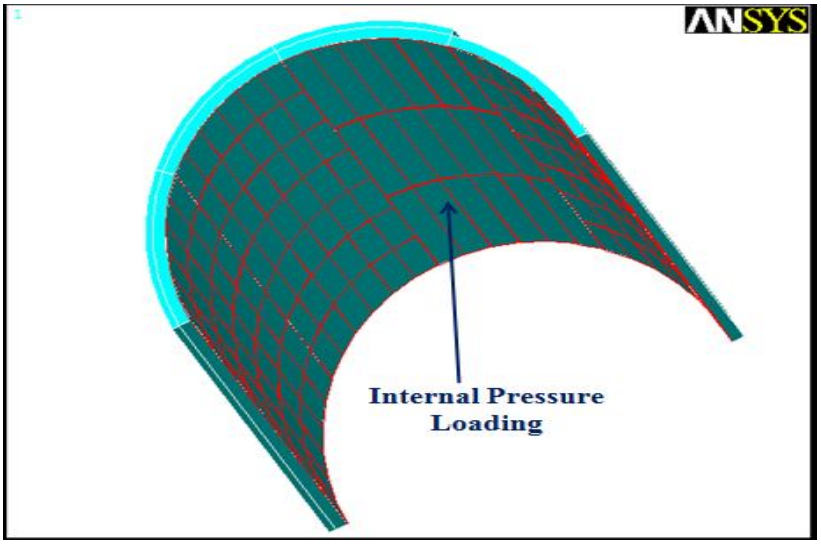

Figure 3.19: Applying Internal Pressure Loading

CHAPTER FOUR

RESULTS AND DISCUSSIONS

4.1 Failure Pressures for Burst Test, Burst Test with Safety Factor, ASME B31G and DNV-RP-F101

The failure pressures for Actual Burst Test, Burst Test with Safety Factor, ASME B31G and DNV-RP-F101 are shown in **Table 4.1**. After calculating the failure pressure using ASME B31G and DNV-RP-F101 codes, the failure pressure values for every model are determined by ANSYS. The safety factor used for Burst Test with Safety Factor, ASME B31G and DNV-RP-F101 is 0.72. The models are simulated with varying internal pressure loading, P_{burst} to achieve the Von Mises Stress values that equal the Specified Minimum Tensile Strength, SMTS of the pipe, which is 455MPa.

Table 4.1: Failure Pressures for Burst Test, Burst Test with Safety Factor, ASME B31G and DNV-RP-F101

Model	Actual Burst Test (MPa)	Burst Test with Safety Factor (MPa)	ASME B31G (MPa)	DNV-RP-F101 (MPa)
Model 1	38.50	27.72	23.05	22.14
Model 2	38.50	27.72	19.03	13.60
Model 3	38.50	27.72	21.74	21.60
Model 4	38.50	27.72	21.74	21.60
Model 5	38.50	27.72	19.03	13.60
Model 6	38.50	27.72	20.26	17.35
Model 7	38.50	27.72	20.26	17.35
Model 8	38.50	27.72	21.00	13.50

4.2 ANSYS Results

4.2.1 Model 1: Average Defect Throughout

The iterations of failure pressure are tabulated in **Table 4.2** and the final result is illustrated in **Figure 4.1**.

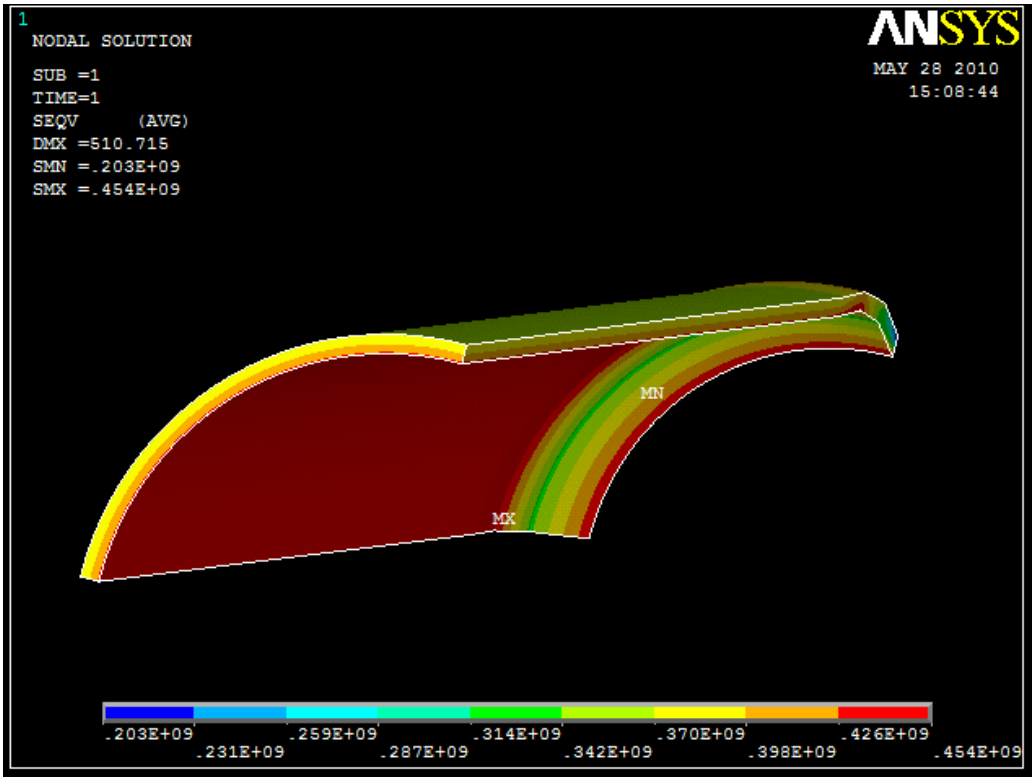

Figure 4.1: Von Mises Stress Plot for Model 1

Table 4.2: The simulation results for Model 1

Trial	Internal Pressure Loading (MPa)	Axial Loading (MPa)	Von Mises Stress (MPa)
1	19.00	108.46	219
2	25.00	142.71	288
3	**39.43**	**225.08**	**455**

4.2.2 Model 2: External Defect Throughout, Width A

The iterations are tabulated in **Table 4.3** and the final result is illustrated in **Figure 4.2**.

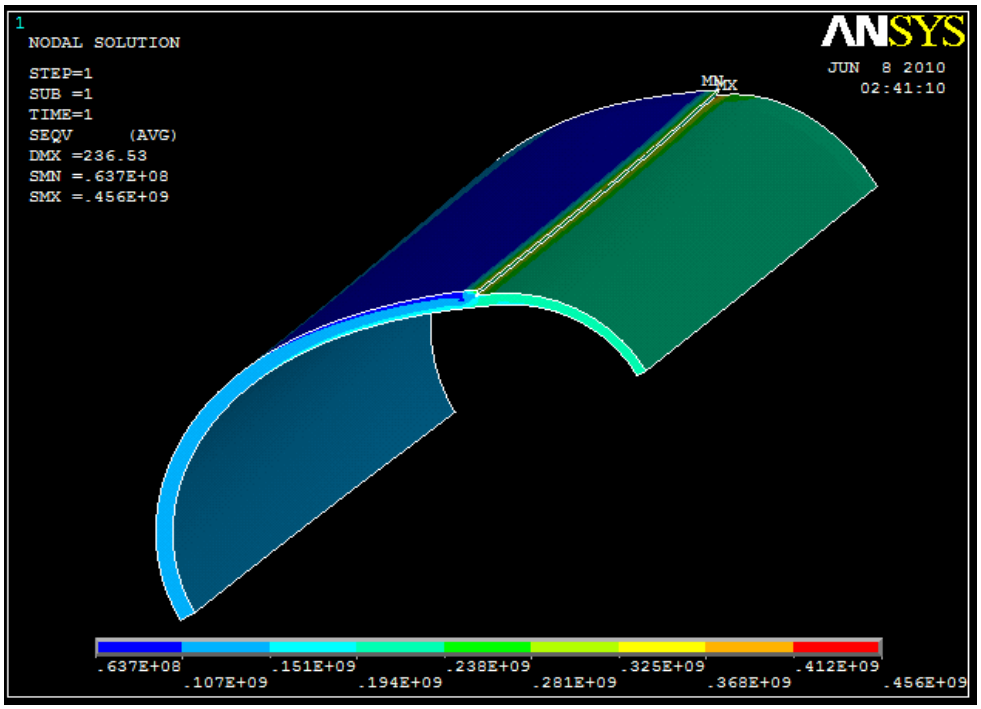

Figure 4.2: Von Mises Stress Plot for Model 2

Table 4.3: The simulation results for Model 2

Trial	Internal Pressure Loading (MPa)	Axial Loading (MPa)	Von Mises Stress (MPa)
1	19.00	108.46	389
2	19.50	111.31	399
3	**22.24**	**126.95**	**455**

From the simulation result in **Figure 4.2**, the high stress area is observed at the corner of the defect.

4.2.3 Model 3: External Corrosion Pit, Geometry A

The iterations are tabulated in **Table 4.4** and the final result is illustrated in **Figure 4.3**.

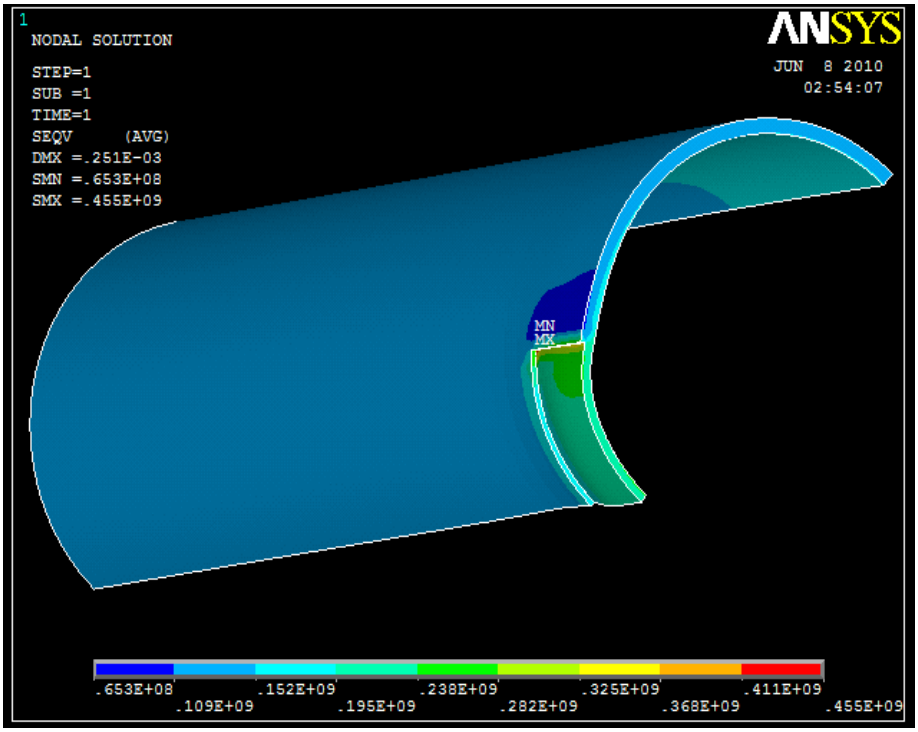

Figure 4.3: Von Mises Stress Plot for Model 3

Table 4.4: The simulation results for Model 3

Trial	Internal Pressure Loading (MPa)	Axial Loading (MPa)	Von Mises Stress (MPa)
1	19.00	108.46	386
2	19.50	111.31	396
3	**22.40**	**127.87**	**455**

Figure 4.3 shows the result from the simulation. The high stress area is observed at the corner of the defect.

4.2.4 Model 4: Internal Corrosion Pit, Geometry A

The iterations are tabulated in **Table 4.5** and the final result is illustrated in **Figure 4.4**.

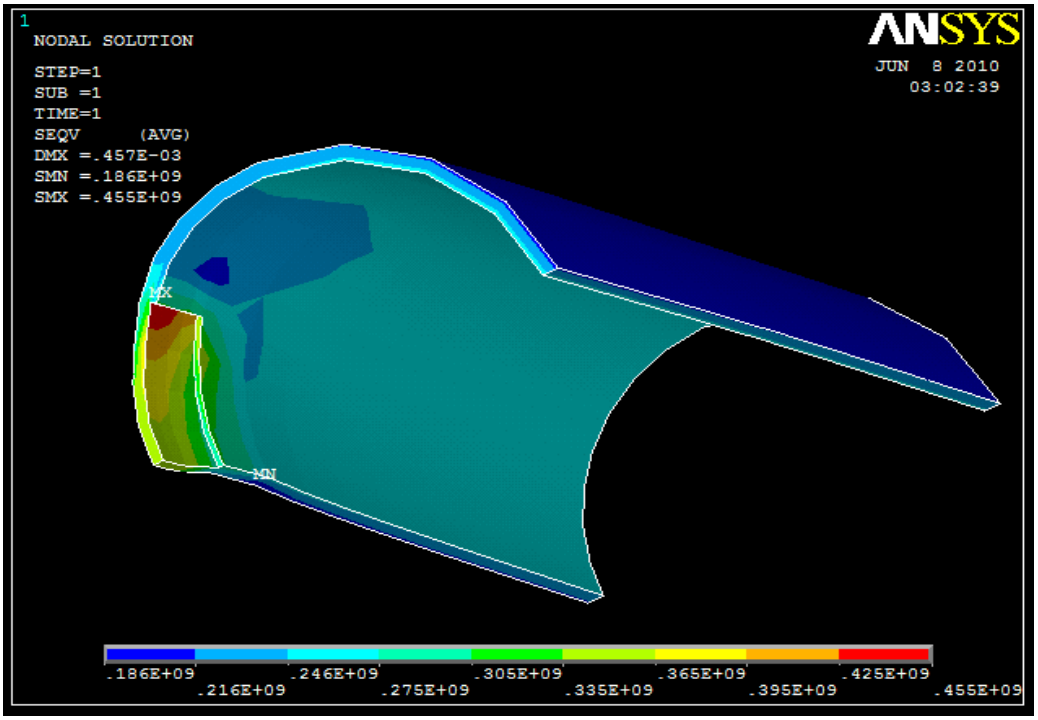

Figure 4.4: Von Mises Stress Plot for Model 4

Table 4.5: The simulation results for Model 4

Trial	Internal Pressure Loading (MPa)	Axial Loading (MPa)	Von Mises Stress (MPa)
1	19.00	108.46	361
2	19.50	111.31	370
3	**23.98**	**136.89**	**455**

From the simulation result in **Figure 4.4**, the high stress area is observed at the corner of the defect.

4.2.5 Model 5: External Defect Throughout, Width B

The iterations are tabulated in **Table 4.6** and the final result is illustrated in **Figure 4.5**.

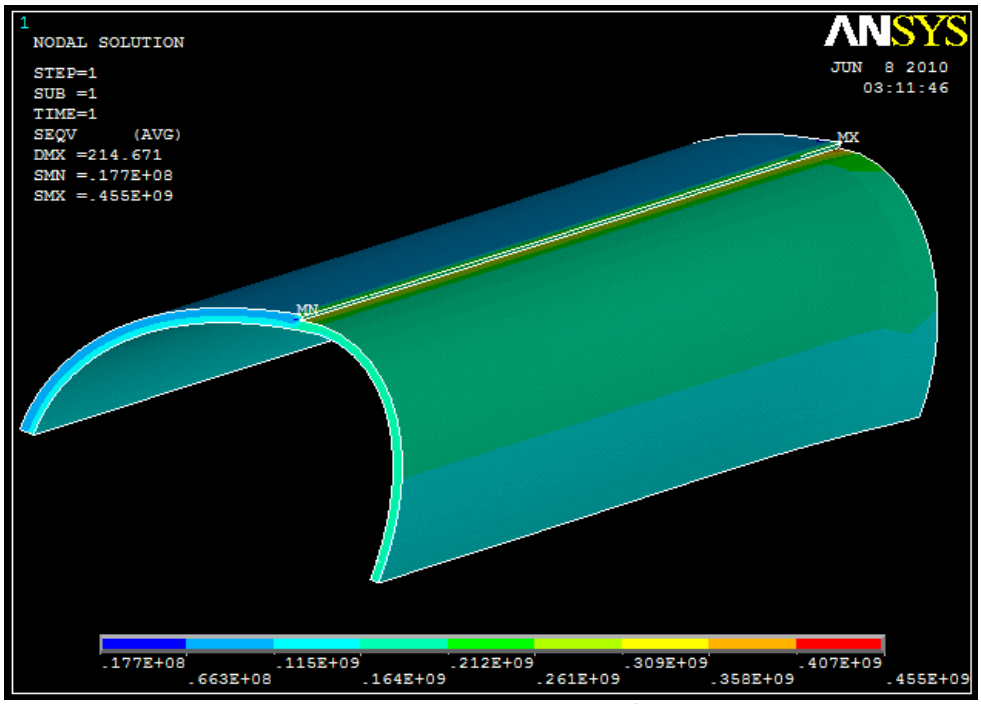

Figure 4.5: Von Mises Stress Plot for Model 5

Table 4.6: The simulation results for Model 5

Trial	Internal Pressure Loading (MPa)	Axial Loading (MPa)	Von Mises Stress (MPa)
1	19.00	108.46	408
2	19.50	111.31	419
3	**21.18**	**120.90**	**455**

From the simulation result in **Figure 4.5**, the high stress area is observed at the corner of the defect.

4.2.6 Model 6: External Corrosion Pit, Geometry B

The iterations are tabulated in **Table 4.7** and the final result is illustrated in **Figure 4.6**.

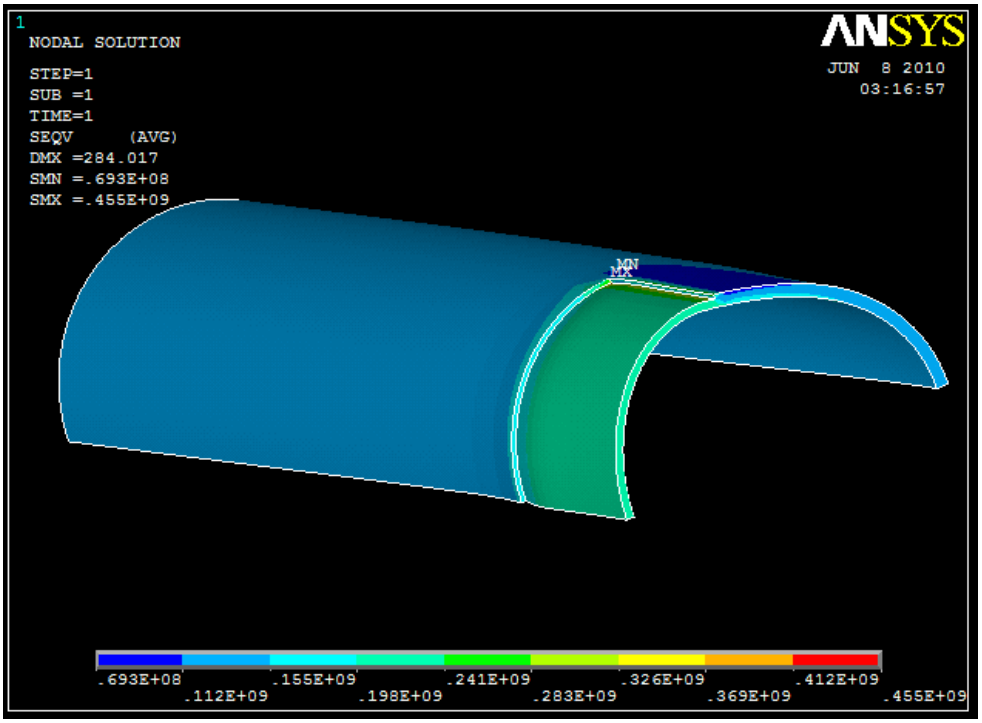

Figure 4.6: Von Mises Stress Plot for Model 6

Table 4.7: The simulation results for Model 6

Trial	Internal Pressure Loading (MPa)	Axial Loading (MPa)	Von Mises Stress (MPa)
1	19.00	108.46	363
2	19.50	111.31	373
3	**23.79**	**135.80**	**455**

From the simulation result in **Figure 4.6**, the high stress area is observed at the corner of the defect.

4.2.7 Model 7: Internal Corrosion Pit, Geometry B

The iterations are tabulated in **Table 4.8** and the final result is illustrated in **Figure 4.7**.

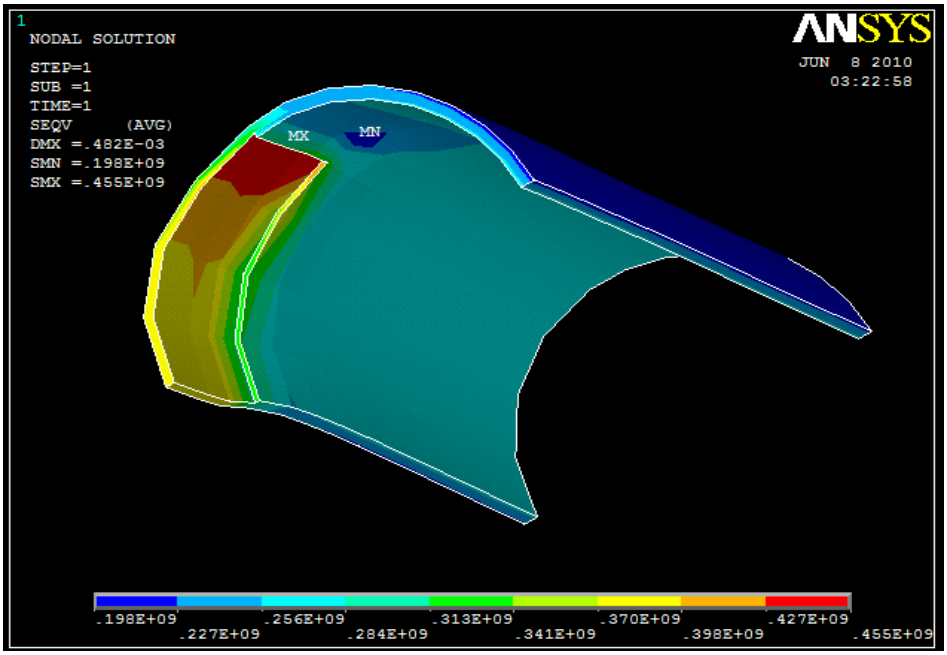

Figure 4.7: Von Mises Stress Plot for Model 7

Table 4.8: The simulation results for Model 7

Trial	Internal Pressure Loading (MPa)	Axial Loading (MPa)	Von Mises Stress (MPa)
1	19.00	108.46	343
2	19.50	111.31	352
3	**25.20**	**143.85**	**455**

From the simulation result in **Figure 4.7**, the high stress area is observed at the corner of the defect.

4.2.8 Model 8: External Rectangular Corrosion Pits, Geometry A and Geometry B

The iterations are tabulated in **Table 4.9** and the final result is illustrated in **Figure 4.8**.

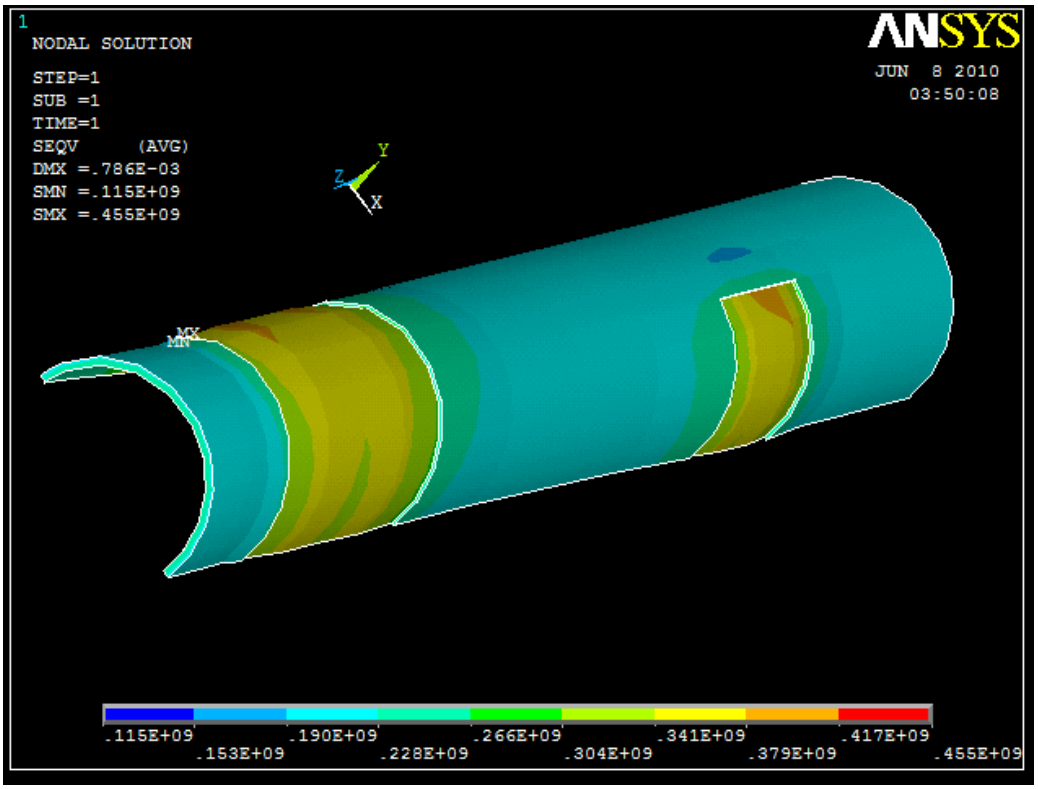

Figure 4.8: Von Mises Stress Plot for Model 8

Table 4.9: The simulation results for Model 8

Trial	Internal Pressure Loading (MPa)	Axial Loading (MPa)	Von Mises Stress (MPa)
1	19.00	108.46	352
2	19.50	111.31	361
3	**25.64**	**146.36**	**455**

From the simulation result in **Figure 4.8**, the high stress areas are observed at the corner of the defects.

4.3 Discussions

The results of each model from the simulations will be tabulated and compared to ASME B31G and DNV-RP-F101, as shown in **Table 4.9**. From the burst test, the Maximum Allowable Burst Pressure (P_b) is found to be 38.5MPa.

The pressure strength of the longitudinal defects is a function of its length, therefore the longer the defect length, *l*, the lower the failure pressure. From the comparisons in **Table 4.9** between Burst Test and Finite Element Analysis, Model 2 (External Defect Throughout, Width A) and Model 5 (External Defect Throughout, Width B) has relatively lower failure pressure. This is due to the corrosion defect throughout the length of the pipe (see **Figure 3.9** and **Figure 3.12**).

Model 3 (External Corrosion Pit, Geometry A) and Model 6 (External Corrosion Pit, Geometry B) have higher error percentage than Model 4 (Internal Corrosion Pit, Geometry A) and Model 7 (Internal Corrosion Pit, Geometry B).

The result for Model 1 (Average Defect Throughout) shows that it has the least error percentage when compared to the actual burst test. From the analysis of the simulation results, the best model that can be used to simulate and evaluate corroded pipe is by averaging the defect depth throughout the corroded profile, as shown in Model 1 (see **Figure 3.8**).

Model 8 (External Rectangular Corrosion Pits Using Geometry A and Geometry B) has lesser error percentage when the Finite Element Analysis (FEA) is compared to the Actual Burst Test, in comparisons to the other models. The simulation results from Model 2 to Model 8 give high error percentages due to the high stress concentration at the corner of the defects of the models. The results can be improved by applying chamfering and filleting to the sharp corners and edges on the defect of the models.

Table 4.9: Comparisons of Failure Pressures

	MODEL 1	MODEL 2	MODEL 3	MODEL 4	MODEL 5	MODEL 6	MODEL 7	MODEL 8
Actual Burst Test	38.50	38.50	38.50	38.50	38.50	38.50	38.50	38.50
Burst Test with Safety Factor (0.72)	27.72	27.72	27.72	27.72	27.72	27.72	27.72	27.72
ASME B31G	23.05	19.03	21.74	21.74	19.03	20.26	20.26	21.00
DNV-RP-F101	23.14	13.60	21.60	21.60	13.60	17.35	17.35	13.50
FEA	39.43	22.24	22.40	23.98	21.18	23.79	25.20	25.64
Error comparisons of DNV to Burst Test with Safety Factor (%)	16.52	50.94	22.08	22.08	50.94	37.41	37.41	51.30
Error comparisons of ASME B31G to Burst Test with Safety Factor (%)	16.85	31.35	21.57	21.57	31.35	26.91	26.91	24.24
Error comparisons FEA to Actual Burst Test (%)	**2.42**	**42.43**	**41.82**	**37.71**	**44.99**	**38.21**	**34.55**	**33.40**

CHAPTER FIVE

CONCLUSION AND RECOMMENDATIONS

5.1 Conclusion

Maximum Allowable Burst Pressure (P_b) is determined from the burst test simulations of corroded pipe using eight different models. The eight models are created in such, so that the best approach to evaluate the remaining strength of a corroded pipe using simulations can be achieved.

Based on the analysis of the simulation results, the Maximum Allowable Burst Pressure (P_b) is 39.43 MPa, and the best approach to evaluate the strength of a corroded pipe is by modelling Model 1, refer **Figure 4.1**. This is because Model 1 gives the least error percentage when its failure pressure determined by Finite Element Analysis (FEA) is compared to Actual Burst Test, refer **Table 4.9**.

In conclusion, in this project, the Maximum Allowable Burst Pressure (P_b) and the best approach to evaluate the remaining strength of corroded pipe are determined from burst test simulations without having to build or destroy prototypes in testing which are very costly.

5.2 Recommendations

Improvements have to be made to the models, especially by adding fillet or chamfering to reduce stress concentration at edges and corners of the defect. The corroded pipe can be idealized into other models that can give better results when compared to the available codes.

More studies are to be conducted to evaluate the Non Linear Finite Element Analysis of Corroded Pipe using burst test simulations.

REFERENCES

[1] Y.T Kho, W.S Kim and Y.P Kim, "*Development of Limit Load Solutions for Corroded Gas Pipelines*", 2002, R&D Centre, Korea Gas Corporation.

[2] Rita C.C Silva, Joao N.C Guerreiro and Patricia R.C. Drach, *"Automatic Finite Element Solid Modelling, Burst and Error Analyses of Corroded Pipelines"*International Journal of Mechanics, Issue 3, Volume 2, 2008.

[3] J.Cappelle,I. Dmytrakh, J. Gilgert, P.Jodin, G. Pluvinage, *"A Comparison Of Experimental Results And Computations For Cracked Tubes Subjected To Internal Pressure"*:2006.

[4] Dr. Clemens Kaminski, "*Stress Analysis & Pressure Vessels*" University of Cambridge, 2005.

[5] Kiefner, J.F and Veith P.H, "*A Modified Criterion for Evaluating the Remaining Strength of Corroded Pipe*", Final Report on Project PR 3-805, Battelle Memorial Institute, Columbus 1989.

[6] Y.K Lee, Y.P Kim, M.W Moon, W.H Bang, K.H Oh and W.S Kim, "*The Prediction of Failure of Gas Pipeline with Multi Corroded Region*", School of Materials Science and Engineering, Seoul National University, and Korea Gas Corporation (KOGAS).

[7] ASME B31G, "*Manual for Determining the Remaining Strength of Corroded Pipeline.*", ASME B31G-1991.

[8] Recommended Practice, Det Norske Veritas, DNV-RP-F101 Corroded Pipelines, October 2004.

APPENDICES

Nomenclatures

A	Projected area of corrosion in the longitudinal plane through the wall thickness (mm^2)
Ac	Projected area of corrosion in the circumferential plane through the wall thickness (mm^2)
D	Nominal outside diameter (mm)
Q	Length correction factor (mm)
SMTS	Specified minimum tensile strength (N/mm^2)
SMYS	Specified minimum yield stress (N/mm^2)
UTS	Ultimate Tensile Strength (N/mm^2)
c	Circumferential length of corroded region (mm)
d	Depth of corroded region (mm) or defect depth (mm)
f_u	Tensile strength to be used in design
l	Longitudinal length of corroded region (mm)
P_{corr}	Allowable corroded pipe pressure of a single longitudinal corrosion defect under internal pressure loading (N/mm^2)
P'	safe maximum pressure for the corroded area
P	greater of either the established MAOP
S	specified minimum yield strength, SMYS (N/mm^2)
ε_d	Factor for defining a fractile value for the corrosion depth
γ_d	Partial safety factor for corrosion depth
γ_m	Partial safety factor for longitudinal corrosion model prediction
F	appropriate design factor from ASME B31.4, ASME B31.8, or ASME B31.11
T	temperature derating factor from the appropriate B31 Code
t	Uncorroded, measured, pipe wall thickness (mm)